AD A137 028 OPTICAL ANALOG & HYBRID COMPUTER SOLUTION OF PARTIAL DIFFERENTIAL EQUATIO..(U) CALIFORNIA UNIV SAN DIEGO LA JOLLA DEPT OF ELECTRICAL ENGINEE.. S H LEE 02 OCT 83 1/1

UNCLASSIFIED AFOSR-TR-83-1296 F49620-83-K-0022 F/G 20/6 NL

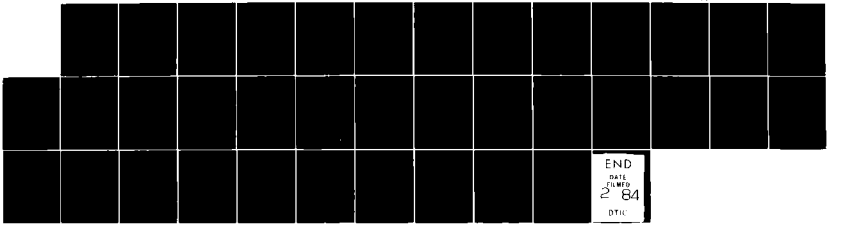

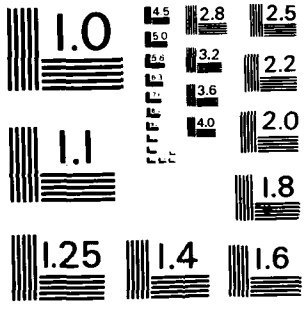

MICROCOPY RESOLUTION TEST CHART
NATIONAL BUREAU OF STANDARDS - 1963 - A

"OPTICAL ANALOG & HYBRID COMPUTER SOLUTION OF PARTIAL DIFFERENTIAL EQUATIONS"

~~ANNUAL~~ Final REPORT

Submitted to

The Air Force Office of Scientific Research

Air Force Systems Command, USAF

prepared under

AFOSR F49620-83-K-0022

January 1 - December 15, 1982

by

Sing H. Lee

Department of Electrical Engineering & Computer Sciences

University of California, San Diego

La Jolla, California 92093

October 2, 1983

REPORT DOCUMENTATION PAGE

READ INSTRUCTIONS BEFORE COMPLETING FORM

1. REPORT NUMBER: AFOSR-TR- 83-1296	2. GOVT ACCESSION NO.: AD A137028
3. RECIPIENT'S CATALOG NUMBER:	
4. TITLE (and Subtitle): OPTICAL ANALOG & HYBRID COMPUTER SOLUTION OF PARTIAL DIFFERENTIAL EQUATIONS	5. TYPE OF REPORT & PERIOD COVERED: 01 JAN 82-15 DEC 82 Final REPORT
	6. PERFORMING ORG. REPORT NUMBER:
7. AUTHOR(s): Sing H. Lee	8. CONTRACT OR GRANT NUMBER(s): F49620-83-K-0022
9. PERFORMING ORGANIZATION NAME AND ADDRESS: University of California, San Diego Department of Electrical Engineering & Cumputer Science La Jolla, CA 92093	10. PROGRAM ELEMENT, PROJECT, TASK AREA & WORK UNIT NUMBERS: 2305/B1 61102F
11. CONTROLLING OFFICE NAME AND ADDRESS: Air Force Office of Scientific Research/NE Building 410 Bolling AFB, DC 20332	12. REPORT DATE: October 2, 1983 13. NUMBER OF PAGES: 33
14. MONITORING AGENCY NAME & ADDRESS(if different from Controlling Office)	15. SECURITY CLASS. (of this report): Unclassified 15a. DECLASSIFICATION/DOWNGRADING SCHEDULE

16. DISTRIBUTION STATEMENT (of this Report)

Approved for public release;
distribution unlimited.

17. DISTRIBUTION STATEMENT (of the abstract entered in Block 20, if different from Report)

18. SUPPLEMENTARY NOTES

19. KEY WORDS (Continue on reverse side if necessary and identify by block number)

20. ABSTRACT (Continue on reverse side if necessary and identify by block number)

ON BACK

The hybrid optical/electronic processing research at UCSD involves several approaches:

(i) Applying digital statistical pattern recognition theory to optical system via the use of computer generated holograms for optical statistical pattern recognition. In this past year another fast algorithm for computing the discriminant functions of the least square linear mapping technigue has been developed. The algorithm is applicable to those images whose pixel statistics are discribable by the first order Markov process, and is at least 20 times faster than previous methods. To extend optical recognition capability to natural color scenes, a color image processing system by VICOM has been purchased in three phases over a three year period. Combining the VICOM system with the existing UCSD hybrid system will provide the U.S. with one of the best hybrid image processing facitities.

(ii) Incorporting image amplifier into an optical feedback system for solving partial differential equations and performing matrix inversion. The feasibilities of attaining these goals have been demonstrated with a dye image amplifier in the past year. However, it is anticipated that much more impressive results can be obtained with photorefractive crystal image amplifier. It is planned for the nest two years to study applying the nonlinear properties of photorefractive crystal for optical realtime processing and to initiate new studies on adaptive and recursive filtering using a hybrid system.

(iii) Producing nonlinear optical devices using silicon and PLZT for nonlinear image processing. On the silicon, conlinear opto-electronic devices such as phototransistor driven threshold or memory devices are designed and fabricated, and on PLZT, electro-optic modulators. The Si-PLZT devices promise to be much faster than the liquid crystal or microchannel plate electro-optic devices.

(iv) Demonstrating the feasibility of hybrid computing using integrated optical and integrated electronic circuits. The important result achieved last is that MOSFET transistors have been fabricated on a laser annealed silicon thin film on LiTaO(3) substrate. Improved reliability in performance can therefore be expected from this new integrated hybrid structure.

I. Introduction

Our research effort at UCSD has been to develop hybrid optical electronic processing systems capable of high speed computing. We have identified several approaches to hybrid processing worthy of intensive study: (1) optical analog/electronic digital hybrids, employing either a coherent optical processor or a confocal optical feedback system, and (2) optical digital (nonlinear)/electronic digital hybrids, employing either optical parallel logic or integrated optical logic devices. These approaches are worthy of intensive study because optical computation offers the unmatched capabilities of parallelism while electronic computation is currently more flexible. Our focus, then, is to combine the powerful features of both optical and electronic computation. In the following discussions we shall report on the status on various aspects of our research.

II. Optical Implementation of Statistical Pattern Recognition

We have begun applying sophisticated digital signal processing theory for statistical pattern recognition to our optical processing system. For example, in the digital processing world, the modified Fukunaga-Koontz transform and the least-squares linear mapping techniques have been proven to be more useful than matched filtering for separating statistical patterns of two and multiple classes, respectively. The cosine transform has also been shown to be valuable in image coding and compression. With the help of computer-generated spatial filters and the coded phase optical processor, which we have developed (see Fig. 1), we have demonstrated these new transforms optically with the significant computational speed benefit inherent to optical parallel processing [1-3]. For example, if the input object contains (1000 x 1000) pixels and the computer generated spatial filter contains 128 multiplexed discriminant functions also of

(1000 x 1000) pixels (derived from the training sets of statistical patterns) for one of the new transforms, we obtain the 128 transform coefficients in the output by performing 1.28×10^{14} mathematical operations in parallel. Recently, we have also optically implemented the Karhunen-Loéve transform. The basis functions (or eigenvectors) of the K-L transform are shown in Fig. 2.

In the coming year we plan to implement other new optical transformations and continue studying more thoroughly those which were just optically implemented. We plan also to assemble a color image processing system so that the color aspect of images can be included in our statistical image recognition studies.

III. Hybrid Iterative Processing

To facilitate hybrid iterative processing we have been working on combining the current capability of computer analyzing optical output with a new capability of computer addressable, coherent optical input. Hence, we designed and constructed a computer controlled CRT with a fiber optic face plate to address a Hughes liquid crystal light valve (Fig. 3). Presently we are evaluating the performance characteristics of this new interface with respect to spatial resolution, spatial distortion (if any), dynamic range (or signal-to-noise ratio), optical coupling efficiency (between the fiber optics plate of CRT to the writing side of the liquid crystal light valve), optical flatness of the read side of the light valve, etc.

An interesting and useful objective of applying hybrid iterative processing will be to study plasma stability or instability, involving the solution of Poisson's equation and the equations of charge motion. Given an initial charge distribution, the optical solution of Poisson's equation will be obtained by the confocal feedback system for the potential distribution. From this potential

distribution, a microcomputer will calculate the electric field and solve the equations of charge motion, finding the displacement of the charges during a small time step Δt, and then generate a new charge distribution (Fig. 4). The process continues by (optically) solving Poisson's equation with this new charge distribution, displacing the charges by the electric field according to the equations of motion again and so on, to stimulate the plasma behavior as a function of time. Figure 5 illustrates still frames from a movie of computer simulation of anomalous plasma diffusion across a magnetic field. (The calculation was performed on a 48 x 48 space mesh or 2000 plasma particles [4].) To go through one iteration of computation for a charge distribution in the space of (1000 x 1000) pixels, it is estimated that our hybrid system will perform more than 100 times faster than a more expensive digital computer (Fig. 6).

To ensure that our confocal feedback system can accommodate at least (1000 x 1000) pixels, optical design has been performed to determine how negative-lens elements can be used to compensate for the aberrations due to the simple positive-spherical surfaces of the confocal feedback mirrors. The two optical systems of Fig. 7 have been investigated where the negative lenses have been incorporated into the spherical mirrors of one system and into the liquid gate holders for the spatial filters in the other. Details of the investigation are given in Ref.[5], where it is concluded that the mangin mirror system of Fig. 7(a) yields better performance. A set of mangin mirrors has been ordered to experimentally verify the optical design.

To ensure that highly accurate solutions of the Poisson's equation can be obtained optically, we have also been studying the incorporation of coherent image amplification into our confocal feedback system. Proper operation of the dye cell for coherent image amplification requires the construction of an

injection locked (folded ring) dye laser. Figure 8 shows our latest design. Since the ring dye laser is longitudinally pumped (by the Phase-R dye laser) eliminating waste normally incurred in the more conventional transverse pumping schemes, an increased output power (15 kW) and an improved locking efficiency (> 90%) were obtained over our earlier results (5kW output, 74% efficiency) reported in Ref. [6]. Furthermore, with the intercavity telescope in the folded cavity expanding the beam and allowing more grating area to be filled, the output is found to concentrate its power in a much narrower spectral width (by an order of magnitude) centering at 6328Å. The increased output power from the folded cavity ring laser combined with its concentration within a narrower spectral width led to a higher amplification factor (10 vs 3.2) and improved signal/noise ratio for coherent image amplification inside the confocal processor [7]. Figure 9 shows a photograph of the set up in Fig. 8.

To ensure temporal compatibility between the confocal optical feedback system and the image carrying pulse input from the injection-locked ring laser system, the transient response of the confocal system has been studied by employing fast electro-optic shutters and photodetectors [8]. This study covered the period of time from the moment the image carrying pulse first entered the confocal system to when steady state operation was established. Light at different points of the 2-D output was measured and displayed on a fast oscilloscope. (The result obtained from this technique is in agreement with that from an inter-cavity technique, in which the entire 2-D optical output as a function of time was obtained by incorporating a linear phase shifting wedge inside the optical processor at one of the Fourier transform locations. Spatial separation of the successive 2-D outputs then corresponds to sequential circulation inside the Confocal Fabry-Perot.)

In the coming year we plan to incorporate the coherent image amplifier into

a coherent feedback processor to solve partial differential equations (as an intermediate step before plasma simulation studies) and to perform matrix inversion. Specifically, the wave equation whose transfer function has a second order singularity will be solved. The image amplifier will provide the extended dynamic range for improving the accuracy of solution. Optical gain will prove to be essential also to an all-optical method for inversion of matrices by compensating for loss in the feedback portion of the optical system. The graduate student on this project is expected to complete his Ph.D. thesis early next year. To continue his work on inversion of large matrices, to execute plasma simulation studies and to extend our research to adaptive and recursive filtering, we shall search for the best candidates to fill two graduate student positions and a post-doctural researcher position.

IV. Nonlinear Optical Devices and Digital Optical Processing

Previously we have made liquid crystal/cadmium sulfide devices for optical parallel logic operations [9]. With optical feedback these liquid crystal devices displayed threshold, bistable or memory characteristics [10]. Lately we have been studying the fabrication of PLZT devices for optical memory and modulation operations. PLZT devices exhibit memory characteristics because they are very good dielectrics. When a voltage is applied to the electrodes across the PLZT, the charges deposited on the PLZT capacitor will stay for a long time (hence memory characteristics) even after the appplied voltage is removed, unless there is leakage at the surface of the PLZT material. PLZT devices exhibit electro-optic modulation characteristics because they are also birefringent. The attractive features of PLZT material are (i) it is available in large areas (up to 4" dia.), (ii) it is operable up to a microsecond speed (hence faster than the millisecond speed of liquid crystal) and (iii) it requires lower voltage to

operate than $LiNbO_3$ (though slightly higher operating voltage than liquid crystal).

In our initial fabrications of PLZT devices, CdS is used as the photodetector because we have much experience with both sputtered and evaporated CdS films. But, sputtered CdS does not normally adhere to PLZT; an interface layer of titanium dioxide was therefore deposited. It was found that titanium dioxide is also useful for encapsulating the finished PLZT device. To deposit aluminum electrodes on PLZT, normal evaporation procedures were followed, except that the PLZT substrate was heated to improve adhesion of the evaporated aluminum onto the substrate. Before the aluminum evaporation, the PLZT substrate must be cleaned; after the aluminum evaporation, the electrode pattern must be etched. Since the PLZT substrates are degradable by acids, normal cleaning and etching procedures must be modified to use basic solutions, e.g., H_2O : NH_4OH : H_2O_2 in a 5 : 1 : 1 ratio. Details of the cleaning and the aluminum electrode deposition procedure are given in Fig. 10.

The PLZT and liquid crystal devices which we are developing can of course be individually employed for nonlinear processing of optical images. A number of them can also be assembled to form a digital optical processing (DOP) system [11]. A DOP contains optical logic and memory devices and electro-optic shutters (Fig. 11) and operates on binary bit planes converted from images (or a 2-D array of numbers). By performing digital (instead of analog) optical processing, we improve the processing accuracy and flexibility while maintaining the parallel processing features inherent to optics. In comparison with digital electronic processing (DEP), we note the following: (1) The degree of parallelism achievable with DOP is far higher than DEP, especially in loading data into and reading data from memory devices. This results from the fact that in a DOP the logic and memory are perpendicular to the data flow while in a DEP the data and

logic reside in the same plane. Hence, the entire image of n x n pixels are operated on optically in parallel, while electronically we expect (in most cases) only an n x 1 parallelism, at least initially even in the Massive Parallel Processor (MPP) [12,13]. The (n x n) vs. (n x 1) parallelism advantage can be utilized in the DOP to minimize the loading and retrieval problem (occurs frequently during the execution of a normal computing program) as well as bypass the substantial integration problem in electronics. (2) Interconnecting optical logic and memory devices with lenses (or holographic optical elements) appears to be far easier than interconnecting electronic parallel logic and memory devices with wires, when the degree of parallelism is high. (3) An optical logic device in a DOP can produce from a pair of binary images two different logic outputs by utilizing two orthogonal polarizations of light. This may help simplify digital system design, e.g., a half-adder circuit can be constructed with two optical parallel logic devices, instead of six as required in conventional electronic design [9]. (4) The power required to perform a logic operation optically on a binary image of n^2 pixels need not be higher than that required to perform the same operation electronically, if the proper kind of opto-electronic devices are used, e.g., devices combining a photoconductor or an array of phototransistors with an electro-optic material [14].

In the past year we have been continuing the construction of the DOP system of Fig. 11, initially with only one memory device (Fig. 12). The optical logic unit (OLU) is identified to consist of two optical parallel logic (OPAL) devices, made of CdS and liquid crystal, and two liquid crystal shutters (S_1 and S_2). Under microprocessor control these two pairs of devices and shutters perform any basic logic operations on inputs I_A, I_B or the readout from the memory (M_1). The resulting OLU output is sent through an editing mask (U_3) to a viewing screen and simultaneously (through a liquid crystal shutter S_{in} under microcomputer control)

to the optical memory (M_1). The memory device currently in use is a liquid crystal OPAL device operated with optical feedback. While information is carried and processed in our system in two-dimensional optical form, control of the various devices and shutters is achieved with an electronic microprocessor. The microprocessor allows the entry of a multiple line "program" for the Digital Optical Processor, translating each code word into a string of binary digits representing those optical devices which are to be turned on or off. These strings are then sequentially directed to an electronic interface to the devices as the programmer's optical algorithm is executed. In Fig. 13 we see the result of computer execution of several steps of a single optical algorithm. After directing the processor to store input "A" in the optical memory and to send input "B" through the logic unit, the picture in Fig. 13(b) was taken which shows the simultaneous output on the memory display screen on the left and the logic display screen on the right. The processor was next directed to erase the memory, calculate and store the logic function A AND B, and then calculate A EXOR B. In Fig. 13(c) we see the results: A AND B on the memory screen, with A EXOR B output through the logic [15].

Since replacing cadmium sulfide by silicon can lead to faster device and system performances, we plan to study in the coming year methods of combining silicon with PLZT for new devices. Specifically, two methods will be studied: (i) flip-chip binding, (ii) laser annealing silicon on PLZT. On the silicon we plan to design an array of simple electronic circuits, each consisting of a phototransistor and a current amplifier driving the capacitive PLZT (electro-optic) modulator load. Figure 14 presents the top view of four unit cells of a device design and the side view of one unit cell. Figure 15 is the electrical schematic of a unit cell. Figure 16 presents the two methods of coupling between the Si phototransistor/driver circuits and the PLZT modulator area. A 3-D view

of our laser-annealing approach appears in Fig. 17.

After we can demonstrate the working of the above device design, which consists of an array of electronic linear circuits, we shall next design new devices which consist of an array of simple electronic nonlinear circuits, e.g., thresholding, static or dynamic rams. Most likely the design and fabrication of these nonlinear opto-electronic devices will be carried out in the year after next. When we can fabricate sufficient number of (say 4 to 6) good nonlinear opto-electronic devices, we shall then use them to construct another DOP system with competitive performance to DEP.

V. Hybrid (IC/IOC) Computing Circuits

Integrated optical circuit (IOC) is known for its high speed capabilities. To take advantage of the speed of IOC logic we study residue arithmetic. The processing algorithm of residue arithmetic offers potential speed advantages because there is no "carry" bit and the computations of all residue moduli can be executed in parallel. Based on a unit cell design which is composed of photodetectors, an electro-optic cut-off switch, channel waveguides and MOSFET loads (Fig. 18), we have configurated modular IOC logic structures for various computational functions (e.g., addition, subtraction, multiplication and division) and for encoding and decoding (see Ref. 16 for details). The photo-detectors and MOSFET loads are fabricated on a silicon substrate, with the channel waveguides and electro-optic cut-off switch on a $LiNbO_3$ substrate. These substrates are subsequently aligned and bonded together physically (Fig. 19). The photo-detectors on silicon pick up the optical signals in $LiNbO_3$. This is called the flip-chip method.

To fabricate the unit cell of Fig. 18 we identified three important areas for development. The first is to fabricate phototransistors whose photosensitive

areas are optimally designed to couple light signals from channel waveguides (Fig. 20). The photoactive region should be small (< 10 μm) to yield high frequency, high gain operations. The operating voltages of phototransistors must also be matched to that of the electro-optic switch. The positive and negative leads across the phototransistor must be on the same side of the silicon substrate to facilitate making ohmic contact with corresponding electrodes of the electro-optic switches on $LiNbO_3$. The second important area for development is to fabricate grating couplers to couple light from channel waveguides to phototransistors. Coupling using gratings can be more efficient than using evanescent field coupling, and would lead to a smaller required photosensitive area on the phototransistor, less stringent contact requirement between the silicon and $LiNbO_3$ substrates, and a higher signal-to-noise ratio. The third area is to bond the silicon substrate onto the $LiNbO_3$ substrate, allowing the electrical signals on the silicon to be transferred to the electro-optic switches on the $LiNbO_3$.

In the past year, we have made the masks for fabricating unit cells of the hybrid (IC/IOC) circuits shown in Fig. 18. Masks for two kinds of photodetectors were designed: one kind for the n^+/p photodiode with depletion mode MOS load (Fig. 21) and the other for $n^+/p/n^+$ photo-effect-transistor (Fig. 20). Figure 22(a) shows the I-V curve of the n^+/p photodiode, indicating a breakdown voltage of about 90 volts. The leakage current at 10 volts reverse bias is 3 nA. (These are very respectable results.) Figure 22(b) shows the I-V curve of the MOSFET, indicating a breakdown at nearly 36 volts. When the photodiode is subjected to the illumination of a pulse of light, the electro-optic electrodes will have a voltage swing of about 36 volts, which is sufficient to operate the E-O cut-off switch. Figure 23 shows the I-V curve of the phototransistor of Fig. 20. The photogain of the phototransistor is about 135, comparing with the same size

photodiode on the same chip. The low breakdown voltage (~ 2 volts) is believed due to surface breakdown along its long length and the strong basewidth modulation. A new structure of double diffused lateral npn phototransistors as shown in Fig. 24 has been designed, which will have a moderately high breakdown voltage (~ 30 volts) and still maintain reasonable photogain (~ 100).

In the coming year, we shall fabricate the double diffused phototransistor of Fig. 24. We shall also fabricate grating couplers on $LiNbO_3$ for improved coupling efficiency from optical channel waveguide to phototransistor. Following device and component fabrications, we shall fabricate a few simple modular computing circuits for residue computing. These modular circuits will be evaluated for signal contrast ratio, speed, and electrical and optical power consumption. Based on the performance of the modular circuits, we shall evaluate the approach to residue computing system design against other approaches.

Another specially noteworthy research result obtained recently was our success in fabricating MOSFET transistors on a laser annealed silicon thin film on SiO_2 on $LiTaO_3$ [17]. This approach will offer all the advantages of hybrid (IC/IOC) circuits without having to epoxy bond together a silicon and a $LiTaO_3$ substrate. Improved reliability in performance can therefore be expected from this new integrated hybrid structure. The graduate student on this project anticipates completing his Ph.D. thesis in the coming year.

References

1. S. H. Lee, "Optical Recognition of Statistical Patterns." Proceedings of a NASA Conference on Optical Information Processing for Aerospace Applications, Hampton, Virginia (Aug. 18, 1981).
2. Z. H. Gu, J. R. Leger and S. H. Lee, "Optical Implementation of the Least Squares Linear Mapping Techniques." J. Opt. Soc. Am., 72(6):787-793 (June, 1982).
3. J. R. Leger and S. H. Lee, "Optical Implementation of the Fukunaga-Koontz Transform." J. Opt. Soc. Am., 72(5):555-564 (May, 1982).
4. R. W. Hockney, "The Potential Calculation and Some Application," in Methods in Computational Physics. Vol. 9, B. Alder (Ed.) Academic Press (1970).
5. S. Johnston and S. H. Lee, "An Improved Optical Design for Confocal Optical Feedback Processing System." Appl. Opt., 22(10):1431-1438 (1983).
6. R. P. Akins and S. H. Lee, "Coherent Image Amplification by an Injection Locked Dye Amplifier at 632.8mm." Appl. Phys. Lett. 35:660-663 (1979).
7. R. P. Akins and S. H. Lee, "Incorporation of Gain into a Coherent Optical Processor with Feedback." Presented as a poster paper at the 1982 Gordon Conference on Holography and Optical Processing, Plymouth, N.H. (June 12-15, 1982).
8. R. P. Akins and S. H. Lee, "Transient Response and Time Evolutions of 2-D Solutions in a Coherent Optical Processor with Feedback." Appl. Opt., 21(24):4515-4520 (1982).
9. R. Athale and S. H. Lee, "Development of an Optical Parallel Logic Device and a Half-Adder Circuit for Digital Optical Processing." Opt. Eng. 18(5):513-517 (Sept., 1979).

10. R. A. Athale and S. H. Lee, "Bistability and Thresholding by a New Photoconductor Twisted Nematic Liquid Crystal Device with Optical Feedback." Appl. Opt., 20(8):1242-1432 (April 15, 1981).

11. R. A. Athale, H. S. Barr, S. H. Lee and B. J. Bartholomew, "Digital Optical Processing." Proc. SPIE 241:149-152 (1980).

12. K. Batcher, "Design of a Massively Parallel Processor." IEEE Trans. on Comp. C-29:837-839 (1980).

13. D. H. Schaefer, et. al., "The Massively Parallel Processor." AIAA Third Conf. on Comp. in Aerospace, pp. 187-190 (1980).

14. S. H. Lee, "Recent Developments in Optical Information Processing using Nonlinearity and Feedback," in Optical Information Processing, Vol. II, Eds. E. S. Barrekette, Y. E. Nesterikhin, G. W. Stroke and W. E. Kock, Plenum Publishing Corp. (1978).

15. M. Title, H. Barr and S. H. Lee, "Programmable Digital Optical Processing System." Presented as a poster paper at the 1982 Gordon Conference on Holography and Optical Processing, Plymouth, N.H. (June 21-25, 1982).

16. S. Y. Huang and S. H. Lee, "Residue Arithmetic Circuit Design Based on Integrated Optics." SPIE Proc. Vol. 321 (1982).

17. R. E. Reedy and S. H. Lee, "CW Laser Annealing of Silicon Films on $LiNbO_3$ and $LiTaO_3$." Submitted to Applied Physics Letters.

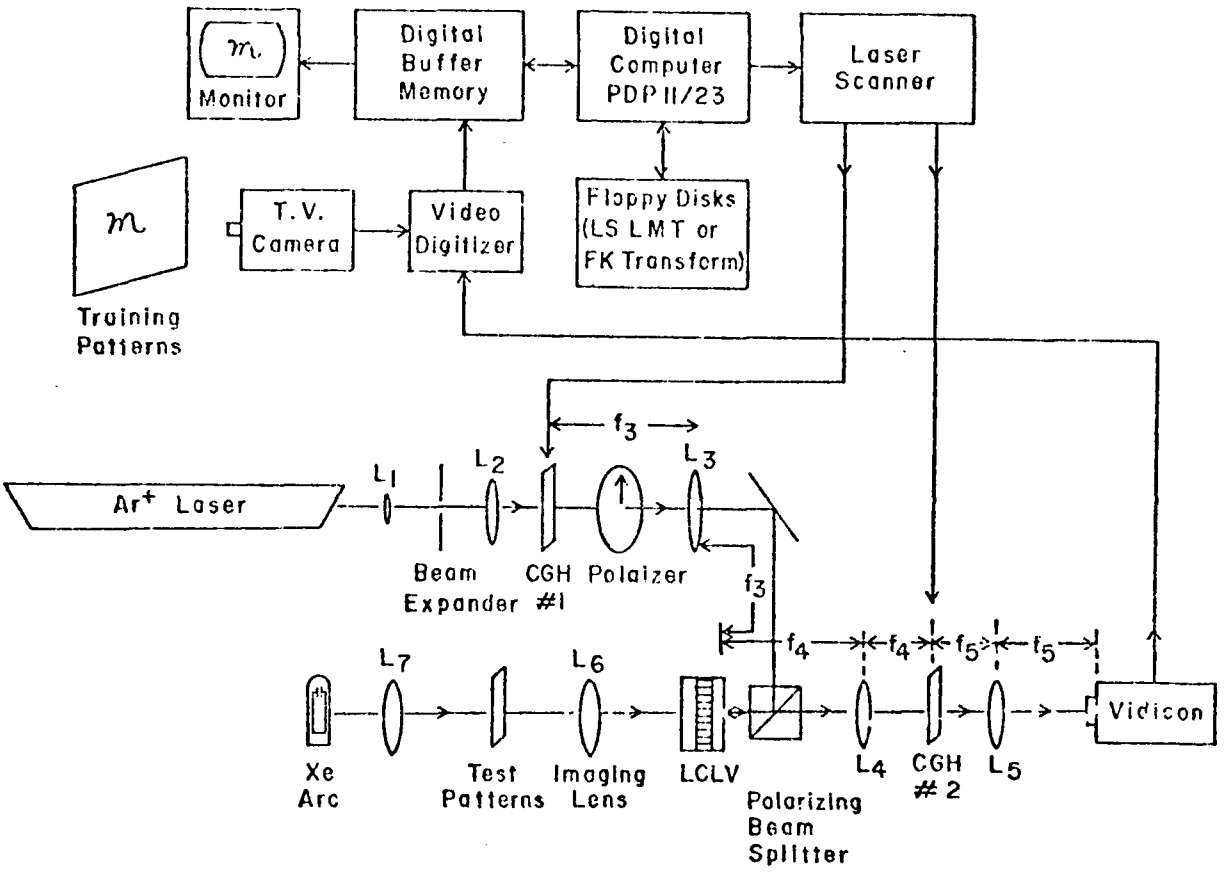

Figure 1. Hybrid implementation of the coded-phase optical processor. A computer generated hologram of a coded-phase array is shown as CGH#1. A second computer hologram containing the F-K or the LSLMT basis functions in coded-phase form is shown as CGH#2. LCLV is a liquid crystal light valve for converting an incoherent (test) image into a coherent image. The resultant F-K or LSLMT coefficients are detected by the vidicon and analyzed by a digital computer. With the same CGH#2 but new test images, new F-K or LSLMT coefficients are obtained and new classifications are achieved in realtime.

Figure 2. The basis functions of Karhunen-Loéve transform for a class of images (birds). Each basis function contains both positive and negative pixels. The grey levels of the small squares next to the basis function numbers indicate the zero levels for that basis function.

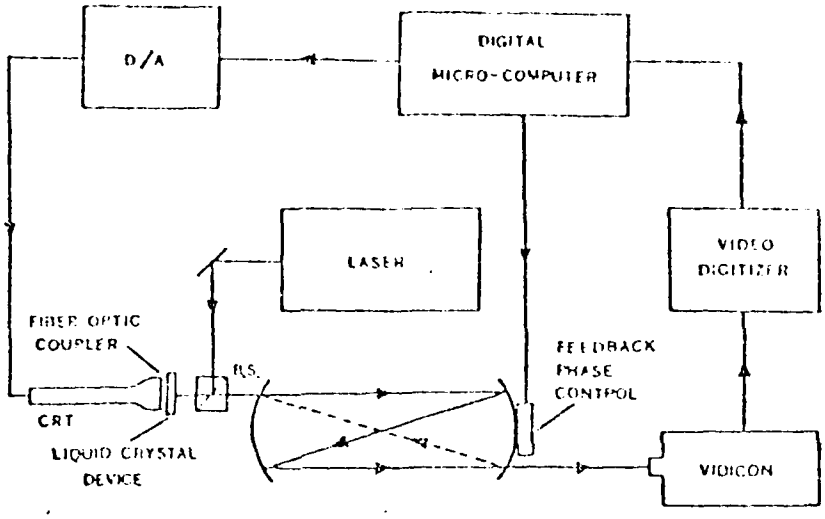

Figure 3a. Schematic diagram showing the microcomputer-controlled video system for real-time image input to coherent optical processor and for real-time analysis of optical output.

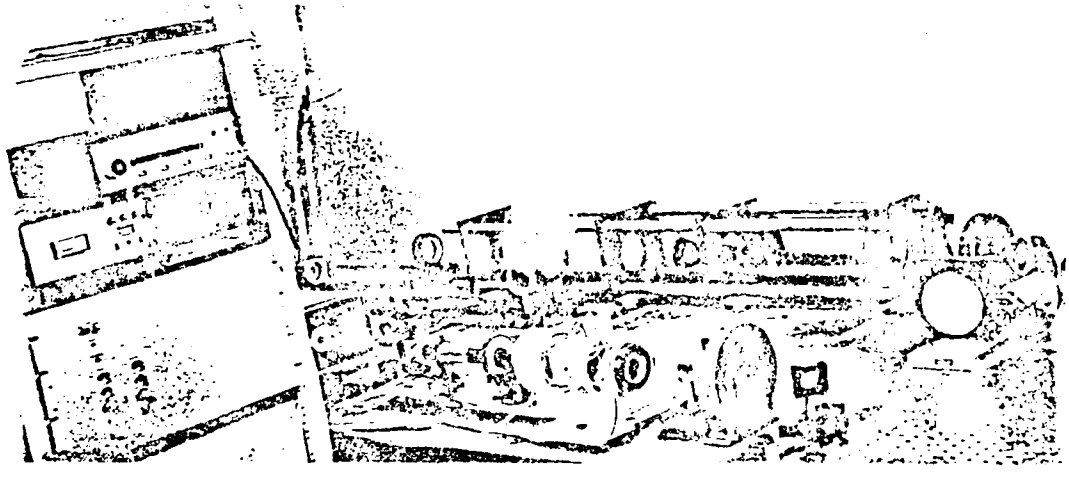

Figure 3b. Photograph of several components of the microcomputer-controlled video system, with the CRT and Liquid Crystal Light Valve in the foreground and the Coherent Optical Processor in the background.

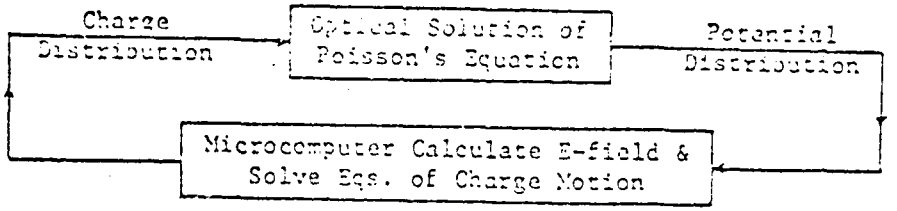

Figure 4. A hybrid iterative processing example for studying plasma stability.

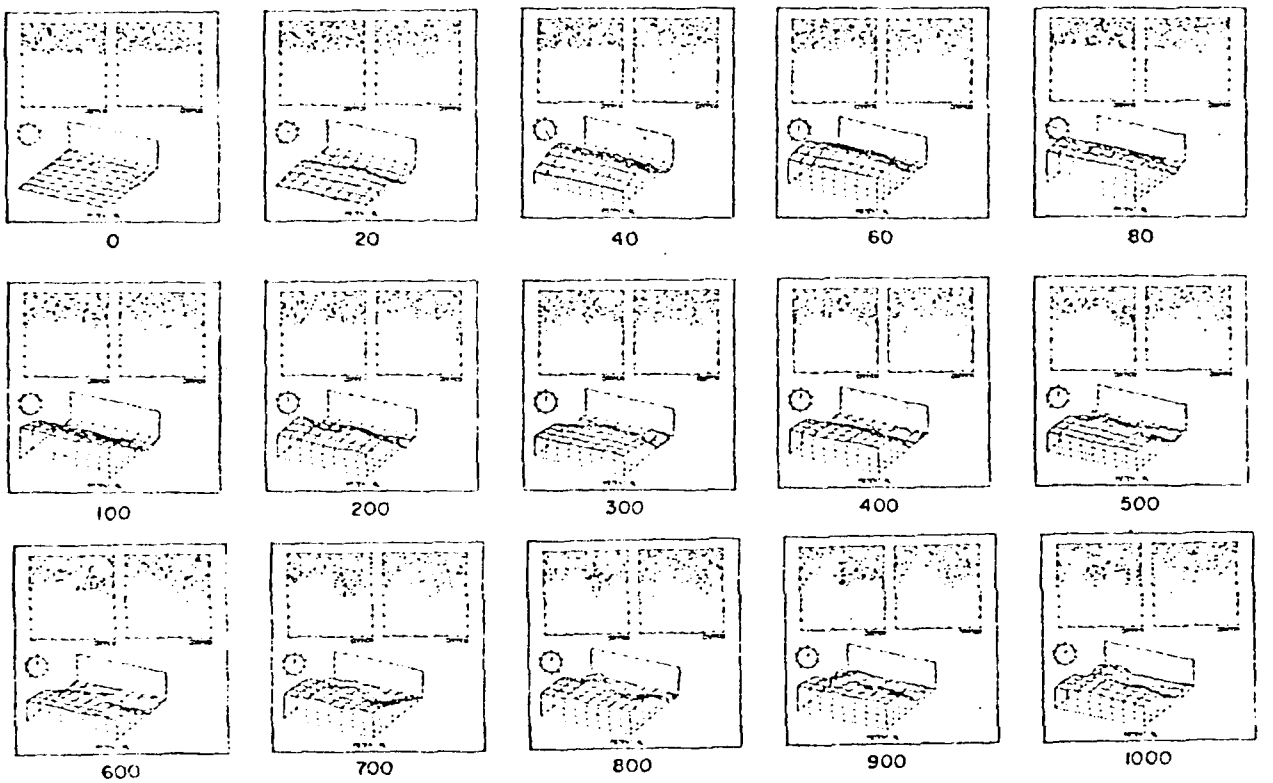

Figure 5. Still frames from a move of the computer simulation of anomalous plasma diffusion across a magnetic field. The electron positions are at the top left and the ions at the top right. Note the formation of a flute in the electron distribution and the growth of a wave on the potential distribution which is shown in projection at the bottom. [p. 188, Ref. 4].

Computing Speed Comparison

1. Solving Poisson's Equation (1000 × 1000 point charges)

   A. Optical Solution
      10 Round Trips in Optical Feedback System — 100 msec
      2 Video Frames — 70 msec ←

   B. Digital Solution on Fast Digital Computer (which take 1 μsec to perform a floating point multiplication followed by an addition) — 125 sec ← ~1785 times

2. One Iteration

   A. Hybrid Solution
      Optical Solution of Poisson's Equation
      Digital Calculation of E-field & Equations of Charge Motion (by microcomputer which takes 120 μsec to perform a floating point multiplication followed by an addition — 1.2 sec ←

   B. Digital Solution — 125 sec ← ~100 times

Figure 6. Computing speed comparison between hybrid iterative processing and digital processing.

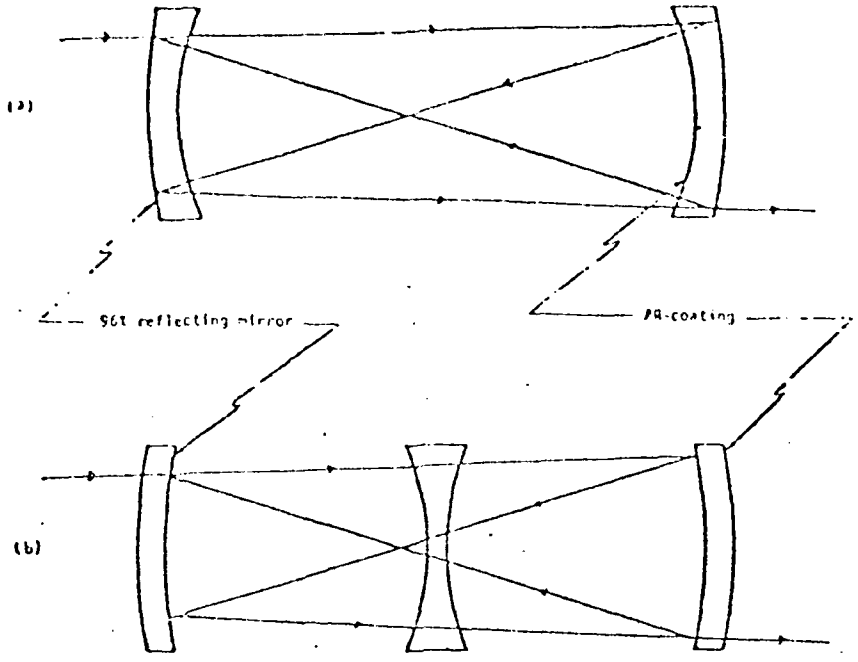

Figure 7. Possible improved designs of the confocal feedback system for increased space-bandwidth product. (a) Negative lenses incorporated into the spherical mirrors by making the radius of curvature of the inner surfaces smaller than that of the outer surfaces. (b) Placing a negative lens in the center of the cavity. This can be done by replacing the optical flats of the liquid gate with planar-concave lenses.

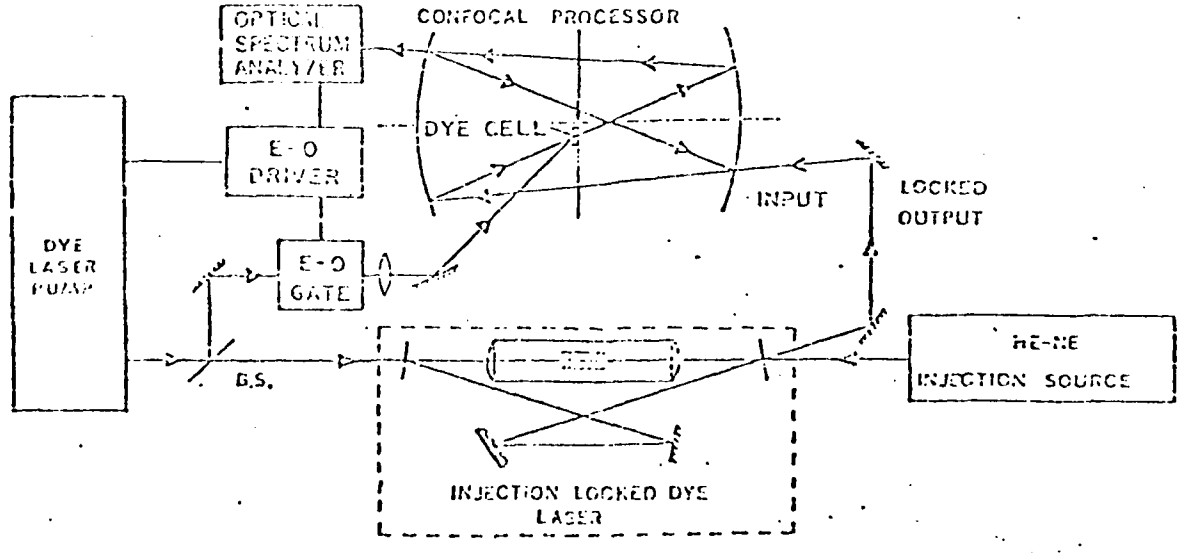

Figure 8. Injection-locked folded cavity ring dye laser and dye (gain) cell for coherent image amplification.

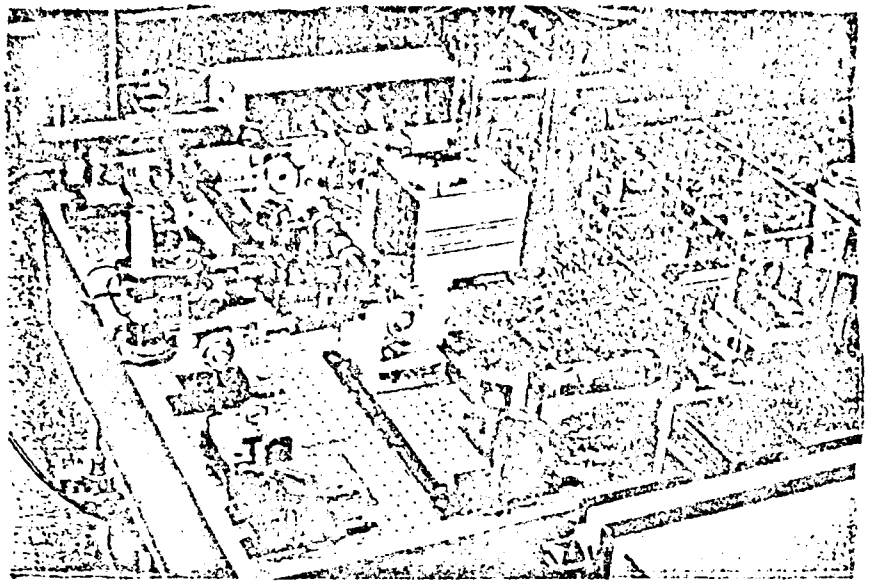

Figure 9. Photograph of the optical system of Figure 8.

I. Substrate Preparation

a) Clean substrate >30 min. in warm (80°C) 5:1:1 solution of H_2O:NH_4OH:H_2O_2. This cleaning procedure is the same as that of normal semiconductor processing except using a basic solution.

b) Rinse >10 min. in running high impedance H_2O; dry substrate.

c) Bake 1 hour 600°C, on clean quartz substrate. Do not allow substrate above 600°C, since this will damage the ceramic.

d) Remove from oven and place in evaporator as quickly and carefully as possible to avoid exposure to environment.

II. Aluminum Deposition

Pump to lower 10^{-6} range; evaporate to opacity. One can heat substrate to improve adhesion of Al layer. This can be done by using internal quartz heater, or IR lamp externally for ≈5 min. prior to evaporation.

III. Photoresist and Etch Step

a) Normal spin but at 4000 RPM, pre-bake 90°C for 30 min. This will yield a photoresist layer thicker than usual.

b) Expose 20 sec.; 1 min. development 1:1 = developer:H_2O.

c) Post-bake 15 min. at 120°C. Post-bake is shorter than usual so that resist can survive boiling Al etch.

d) Etch electrodes in boiling 5:1:1 = H_2O:NH_4OH:H_2O_2 solution. This etch is once again basic solution. Etch until Al layer is properly removed (time can vary).

Fig. 10. Fabrication Procedure: Aluminum electrodes on PLZT.

(a)

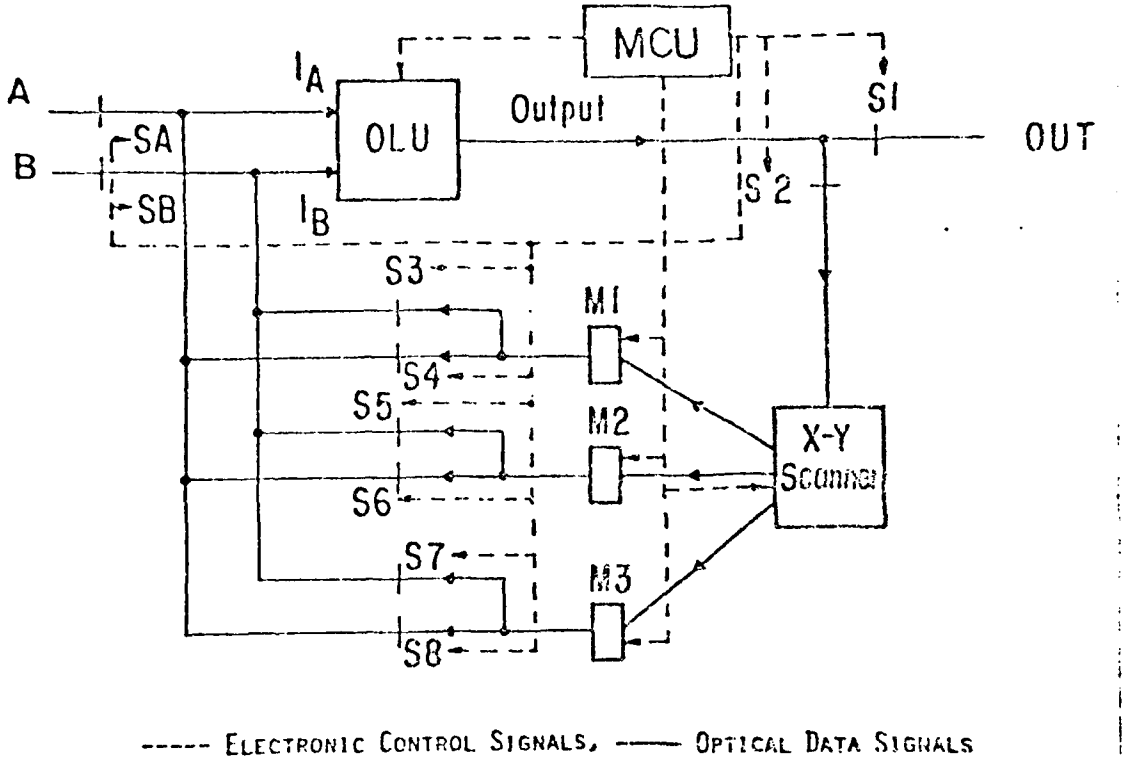

(b)

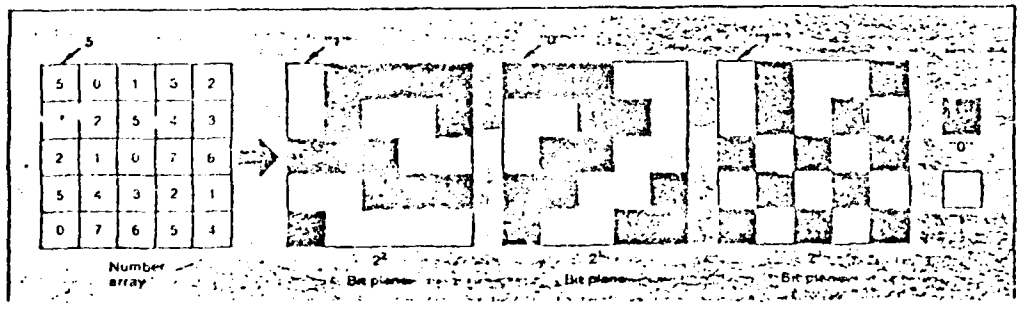

Fig. 11. (a) General schematic of a proposed Digital Optical Processing System. (b) Diagram showing the decomposition of a 2-D analog field into a representation three 2-D bit planes.

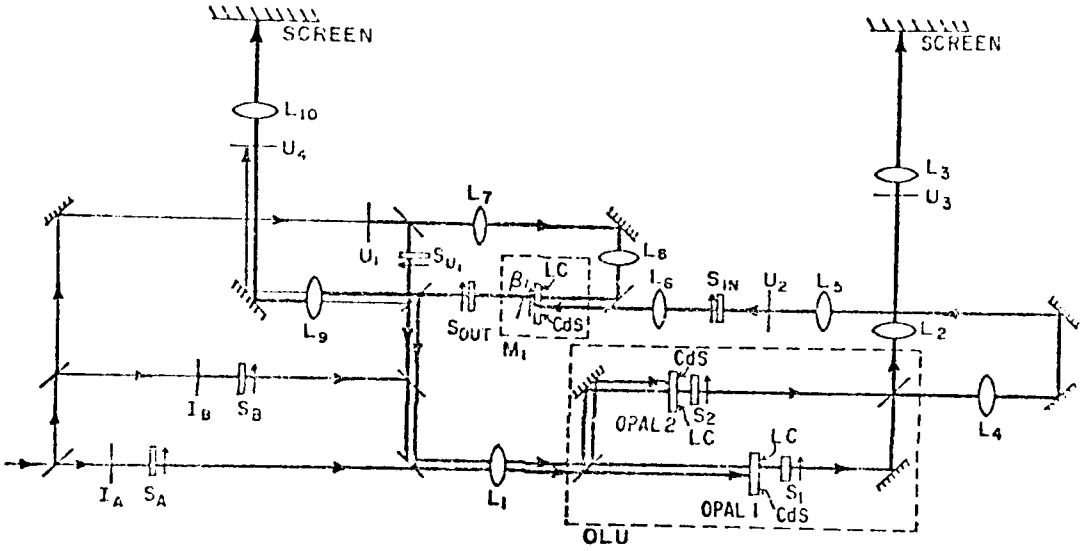

Fig. 12. Schematic of DOP system currently in operation at UCSD. I_A and I_B are inputs, OLU = Optical Logic Unit, and M_1 Optical Memory.

(a)

```
A
STORE
B
ERASE
A AND B
STORE
A EXOR B
:
:
:
```

(b)

(c)

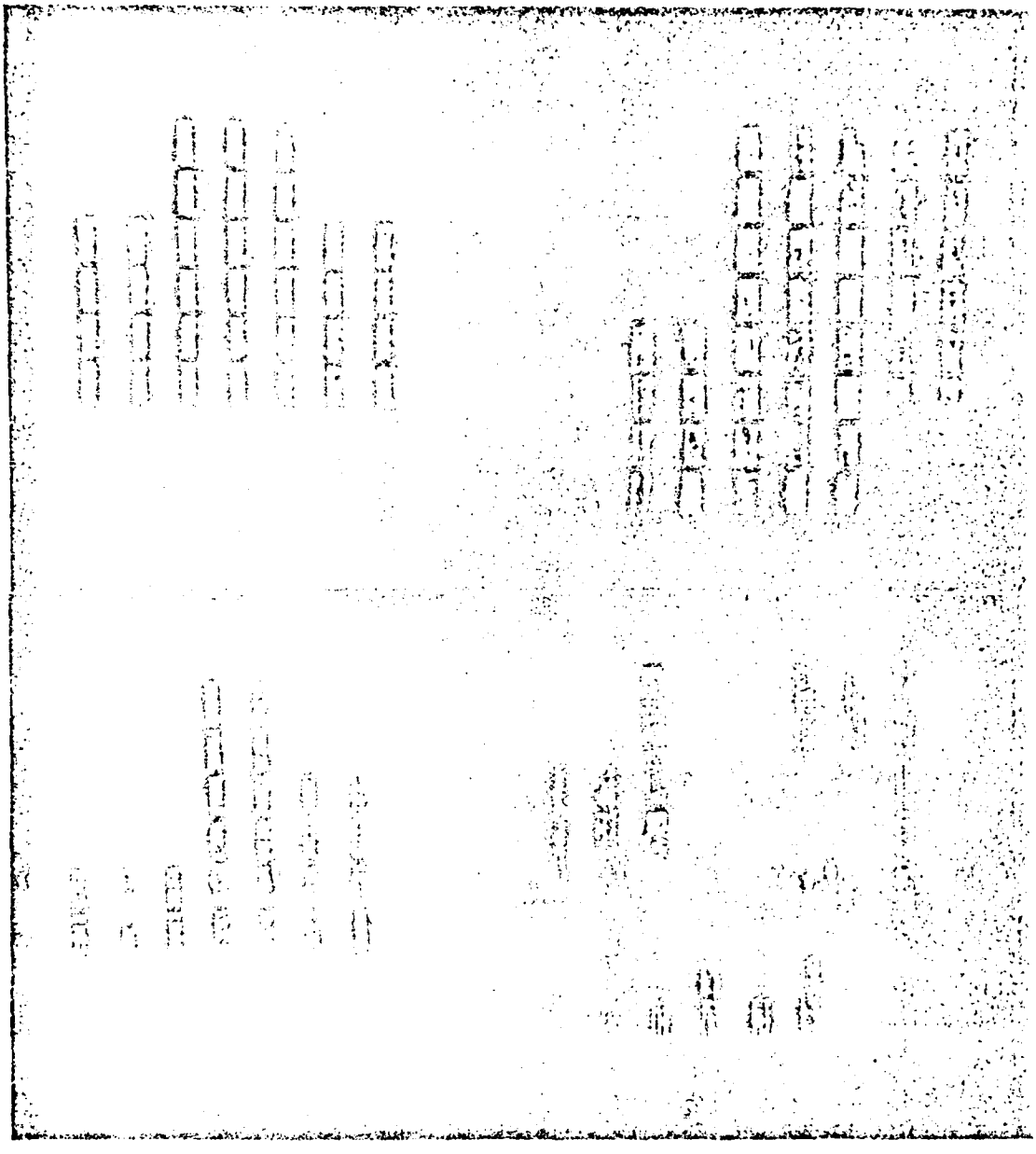

Fig. 13. (a) Sample algorithm executed by DOP system at UCSD. (b) Results of algorithm after first 3 program steps. Memory display is at left, logic display at right. (c) Results after subsequent 4 program steps.

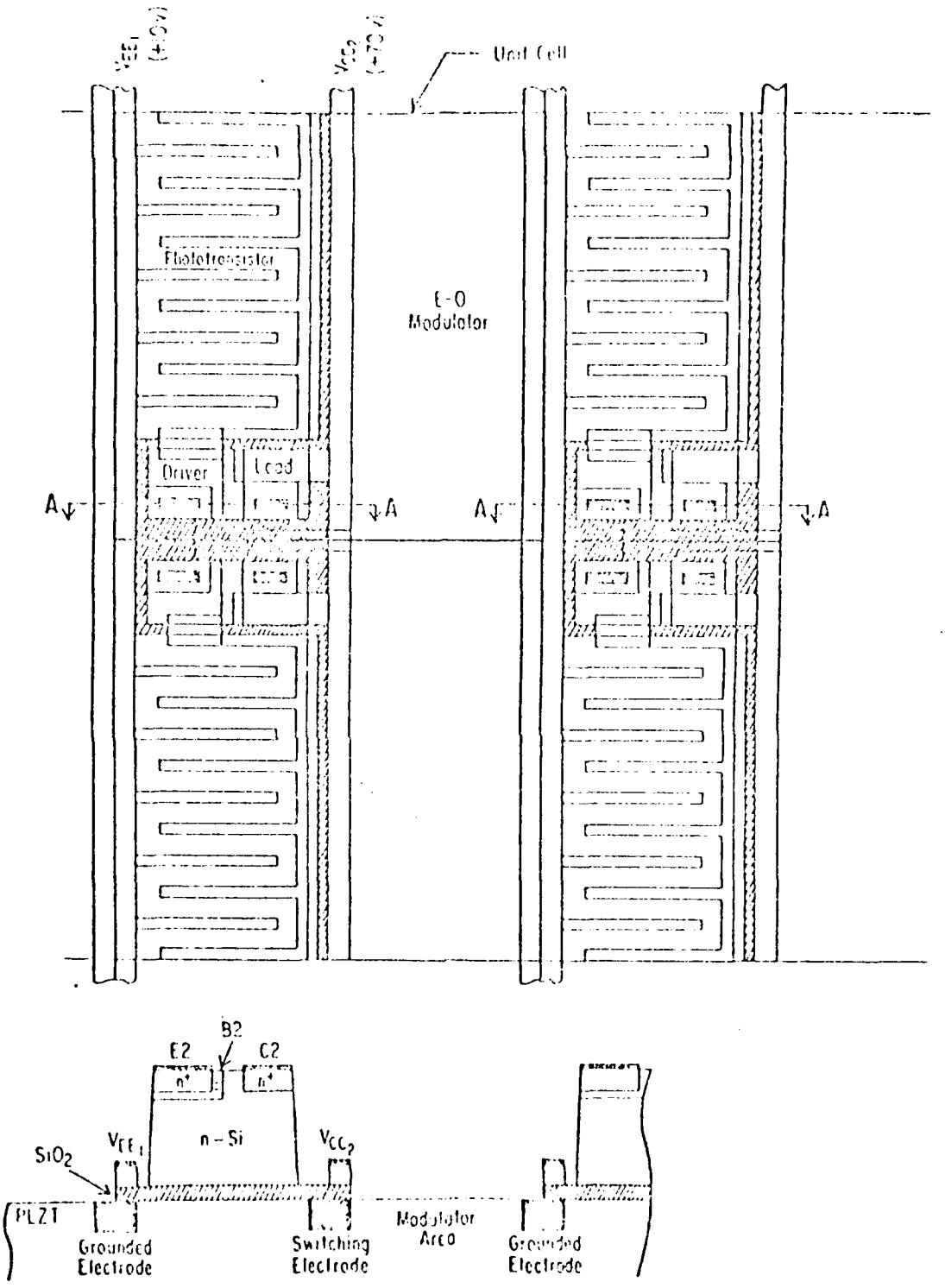

Fig. 14 Top view of four cells and side view at cross-section AA of the Si/PLZT Spatial Light Modulator. The vertical scale in the side view diagram is exaggerated for clarity.

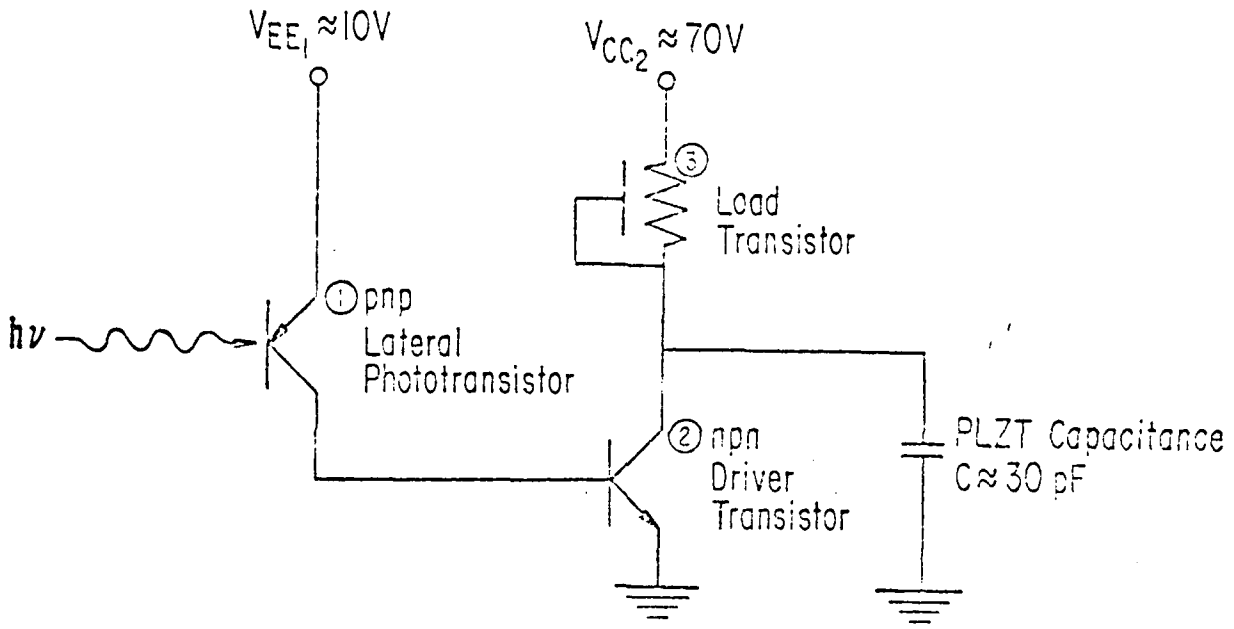

Fig. 15 Electrical circuit of a single cell of the Si/PLZT SLM.

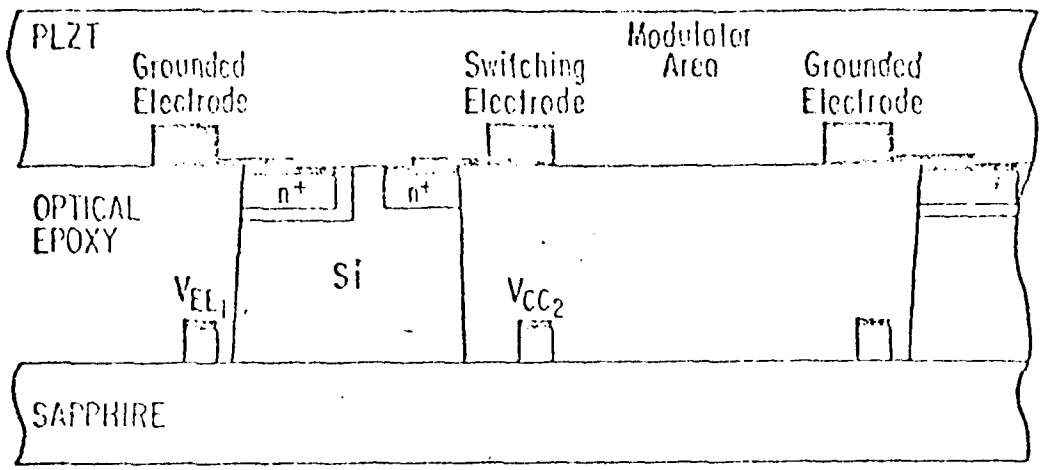

(a)

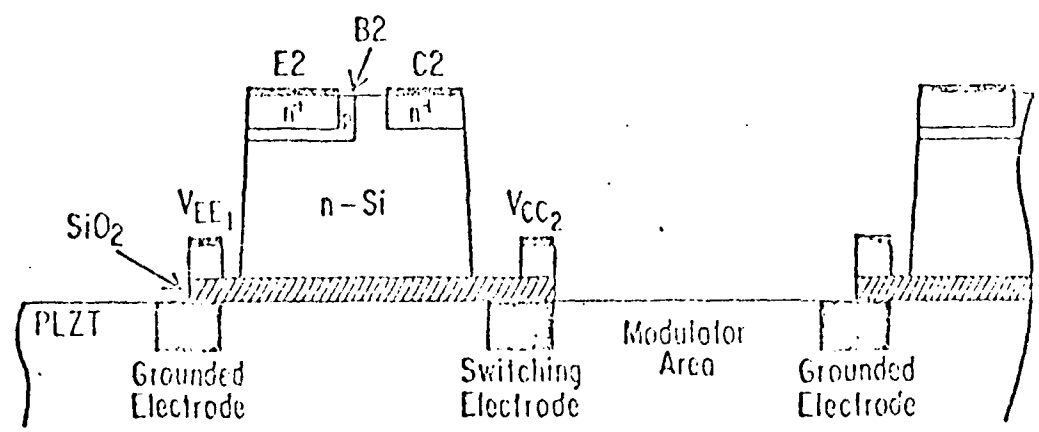

(b)

Fig. 16 (a) Bonded dual-wafer configuration of the Si/PLZT SLM, contrasted with (b) single wafer configuration using laser-annealed Si on Si_2 on PLZT.

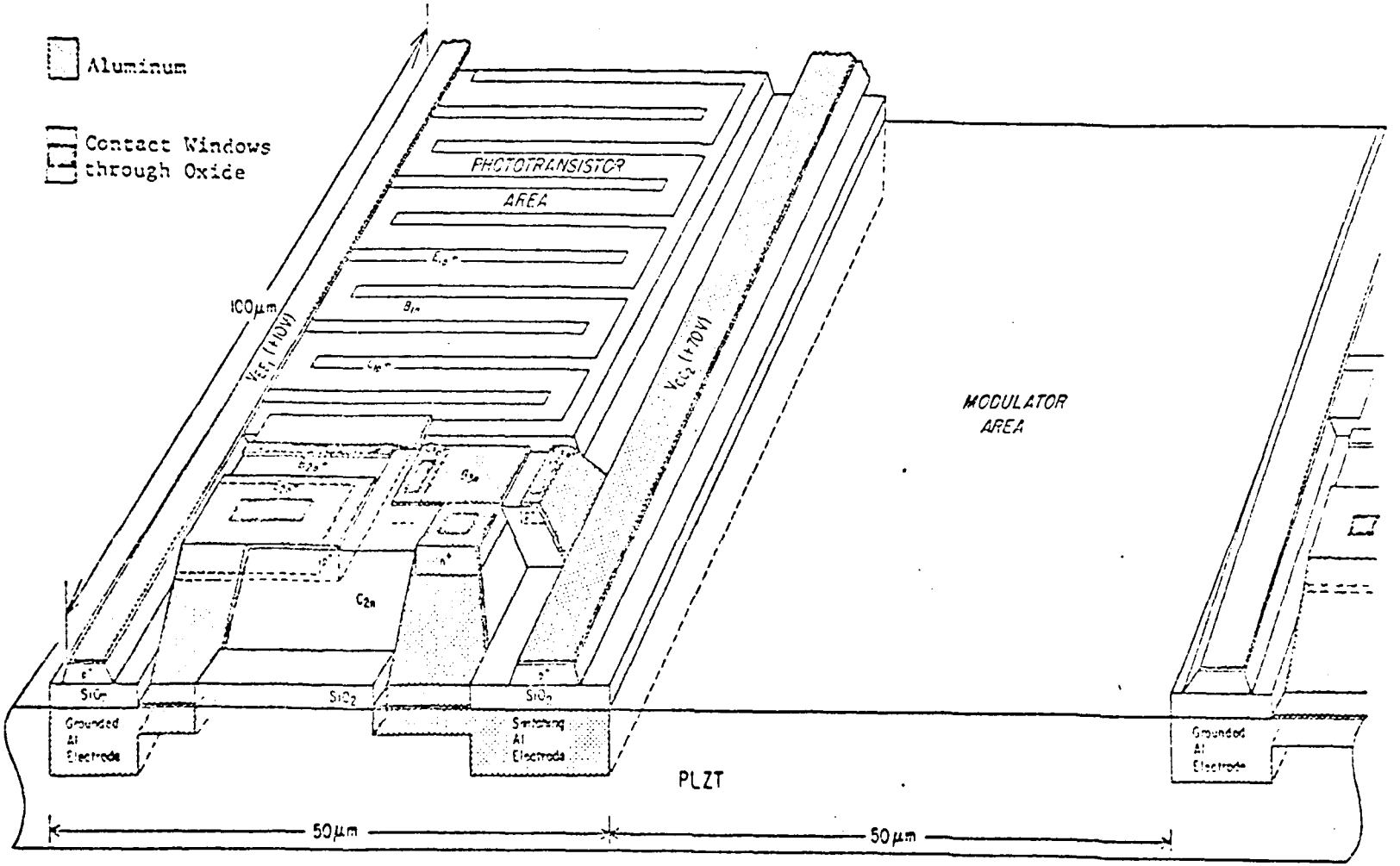

Fig. 17 Three-dimensional view of a unit cell of the Si/PLZT SLM. Vertical scale is exaggerated for clarity. To compare with Figure 5, note connections of the +10V supply (V_{EE_1}) to the p^+ emitter regions (E_1) of the lateral phototransistor (1), and the connection of the phototransistor collector (C_1) to the base (B_2) of the (vertically-structured) driver transistor (2). The driver transistor emitter (E_2) is grounded through contact with the grounded Al electrode in the PLZT. Also note the connection of the +70V supply (V_{CC_2}) to the emitter (E_3) of the lateral load transistor (3), and the connection of the base (B_3) and collector (C_3) of the load transistor to the driver collector (C_2) and to the switching electrode in the PLZT.

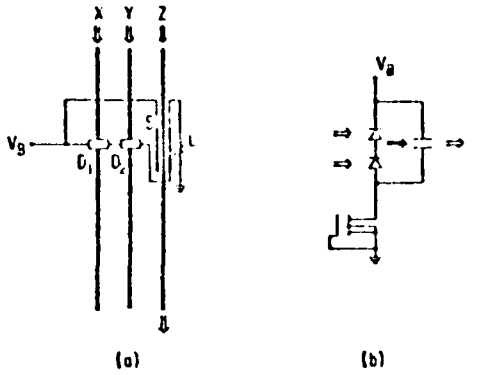

Fig. 18 (a) Schematic diagram, and (b) electrically equivalent circuit of an optically-activated hybrid (IC/IOC) circuit consisting of an E-O cut-off switch S, a MOSFET load L, two photodetectors D_1 and D_2, and three channel waveguides X, Y and Z. ⇒ = cw light. ⇒ = light pulse.

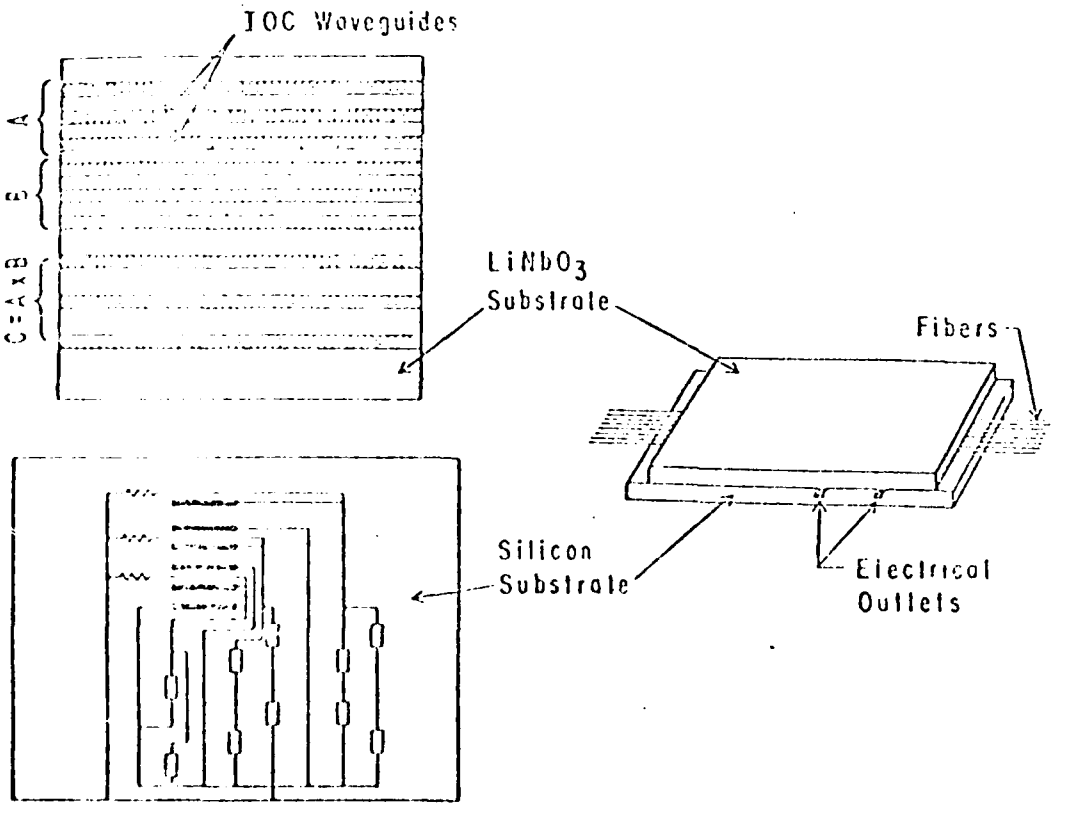

Fig. 19 Flip-chip method of binding, which allows one to interface previously fabricated (a) optical circuits with (b) electrical circuits to produce (c) hybrid circuits as shown schematically on the right.

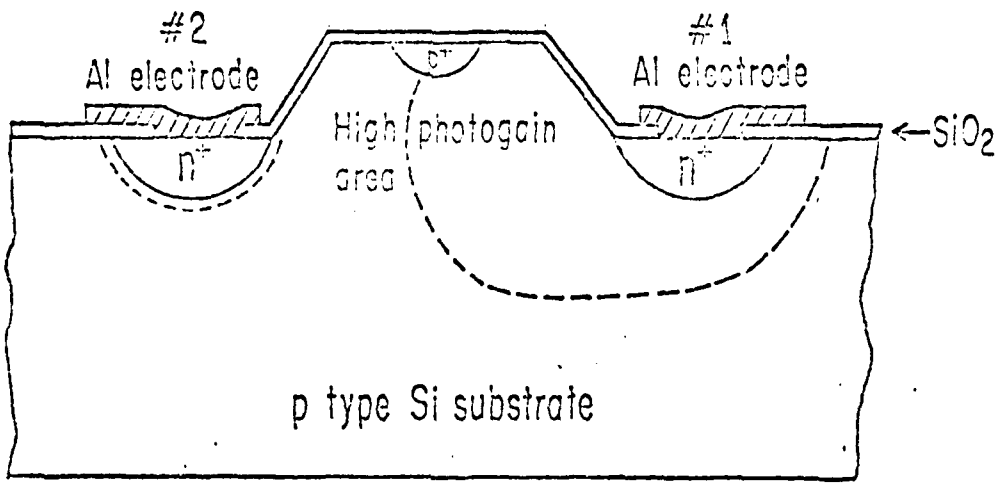

Fig. 20 $n^+/p/n^+$ phototransistors with high photogain and simple structure. Its base is open-circuited. The p^+ doping at the mesa region is for cutting-off the surface leakage current. Dashed lines indicate depletion regions when a positive voltage is applied to the #1 electrode and the #2 electrode is grounded.

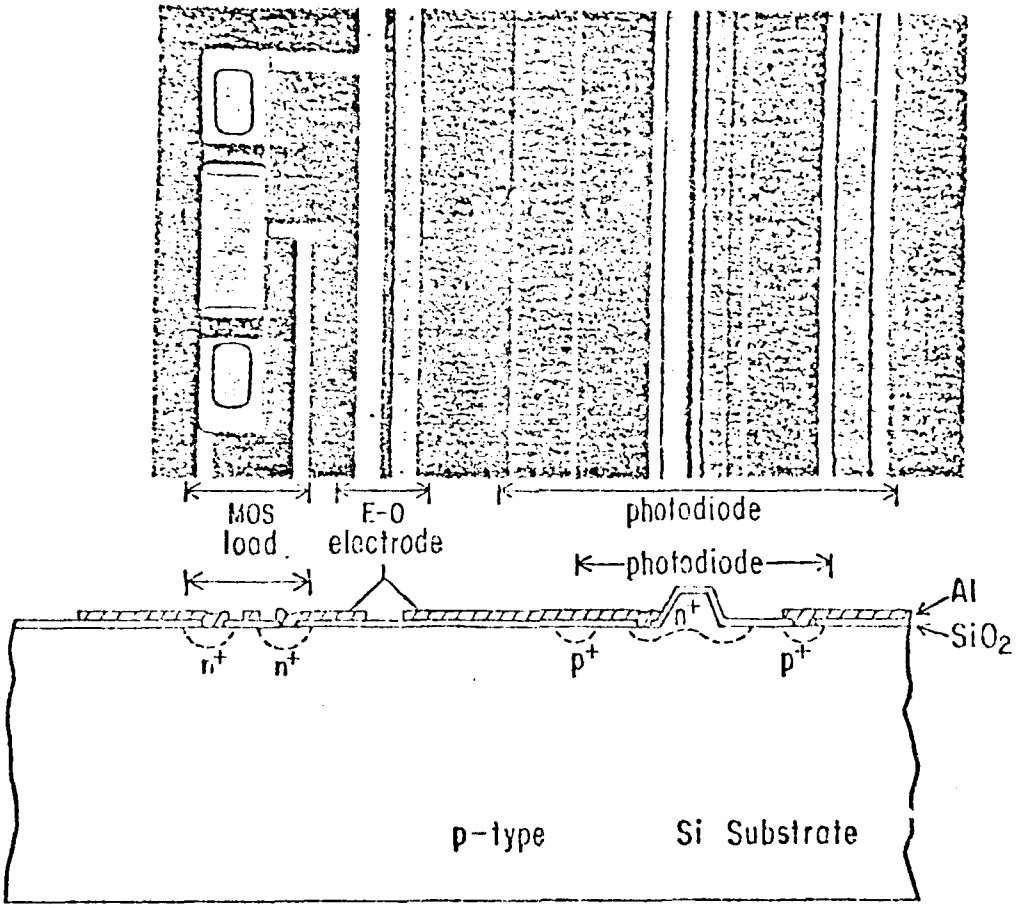

Fig. 21 Combination of n^+/p photodiode, electro-optic electrode and MOS load. The upper picture is top view and the lower one is side view.

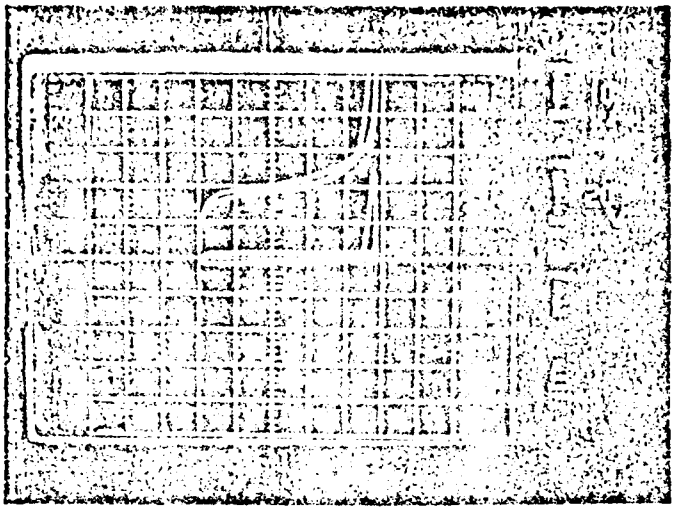

(a)

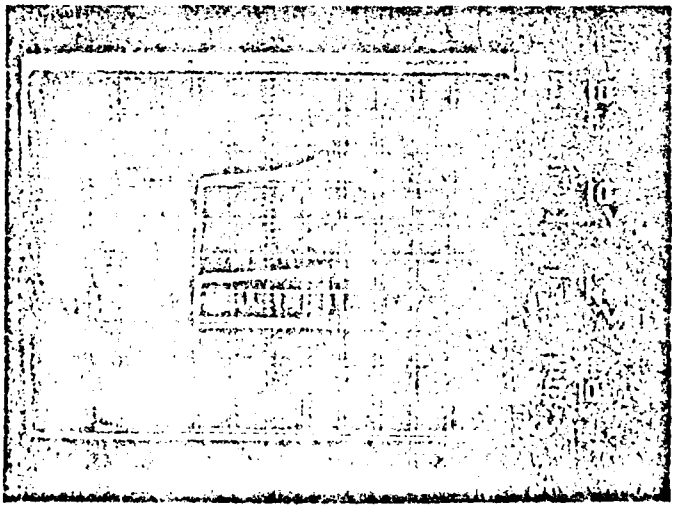

(b)

Fig. 22 (a) The I-V characteristics of the n^+/p photodiode, (b) the I-V characteristics of the MOSFET load shown in Fig. 21.

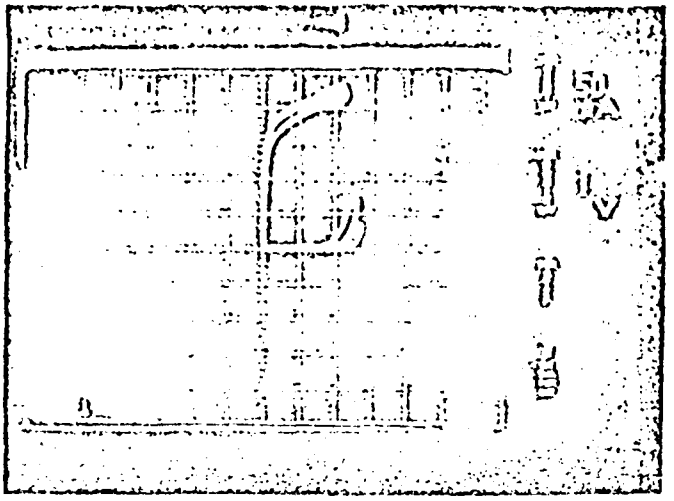

Fig. 23 I-V curve of a lateral npn phototransister measured in the dark (lower curve) and under the illumination (upper curve) of 18 mW/cm^2 white light. The sensitive area of the phototransistor is 8μm x 2000μm.

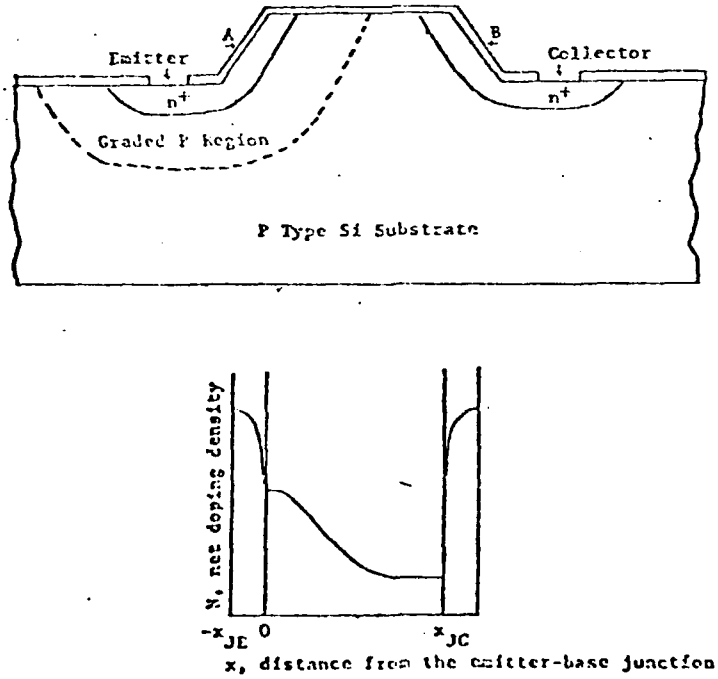

Fig. 24 (a) Cross section of a double diffused lateral npn silicon phototransistor. (b) Impurity profile of the phototransistor along the line $\overline{AB}$.

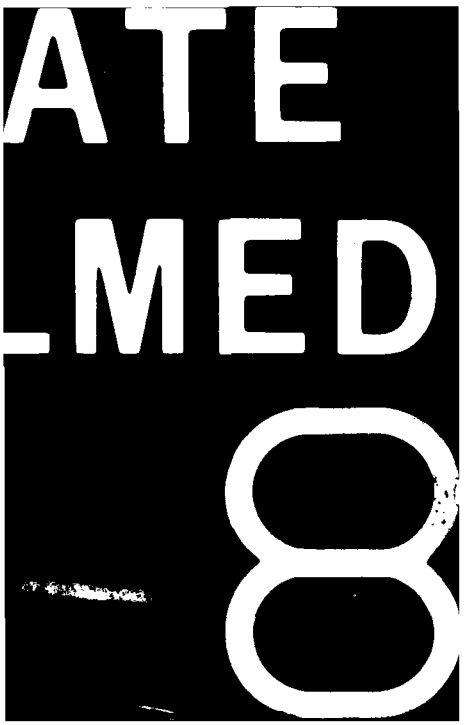
ATE
LMED
8